

Invited paper at 5th Int. Workshop on the Physics
of Semiconductor Devices, New Delhi, Dec 1989

HOLE TRANSPORT AND RELAXATION IN THE VALENCE BAND OF A GaAs-ALAs QUANTUM WELL

R. A. Abram, R. W. Kelsall, R. I. Taylor¹ and A. C. G. Wood
Applied Physics Group
School of Engineering and Applied Science
University of Durham
South Road, Durham, DH1 3LE. UK

There has been much recent experimental and theoretical work on electron dynamics in GaAs based semiconductor heterostructures but the behaviour of holes in these structures has received comparatively little attention.

In a quantum-confined device, the valence band structure consists of a set of discrete subbands, which are strongly mixed in character. We have used a 4-band $k.p$ scheme to model this band structure, for the case of a single GaAs-ALAs quantum well. The dispersion of the subbands in the plane of the well is severely distorted by band-mixing, with regions of negative effective mass and repulsion (anticrossing) between adjacent subbands. The densities of states of these bands show distinct structure, in sharp contrast to the usual step-like form that is often assumed for a two dimensional system. The character of the hole wavefunctions also varies markedly with in-plane wavevector.

We have developed a Monte Carlo simulation of hole transport and relaxation in the quantum well. The model includes the realistic energy bands and phonon scattering due to optical (polar and non-polar) and acoustic (deformation potential and piezoelectric) processes. It is found that the quantum confinement of the hole states causes marked differences in the phonon scattering rates as compared to bulk GaAs. In this paper we describe the physical basis of the Monte Carlo simulation and demonstrate its use in the investigation of the transient energy relaxation of holes in the quantum well and their response to an applied in-plane electric field.

1. INTRODUCTION

A knowledge of the electronic structure of a semiconductor is essential to calculate its electrical and optical properties, or to predict the behaviour of a device made from the material. The calculation of the band structure of bulk semiconductors has been well developed for some time, with a range of techniques available ranging from accurate large scale calculations to more approximate methods that make relatively small demands in terms of

¹. Present address, Plessey Research Caswell Limited, Allen Clark Research Centre, Towcester, Northants, U.K.

computational effort [1]. The advent of low dimensional structures (for example, heterojunction interfaces, quantum wells, and superlattices) has produced new challenges for band structure theorists but an essentially similar picture is emerging as for the bulk, with a range of techniques now available [2].

For the theoretical description of some physical properties the calculation of the electronic structure is the most demanding step. For example the band structure of a GaAs/AlGaAs quantum well is quite complicated with a set of roughly parabolic conduction band subbands for the in-plane E-k dispersion near the zone centre but considerable mixing of the heavy and light hole states occurs and gives rise to a set of highly structured valence subbands which are distinctly non-parabolic [3-5]. However, once the band structure and transition matrix elements are known it is relatively straightforward to determine certain optical properties such as the gain spectrum of a quantum well laser [5], at least if phonon processes and state broadening are neglected. The simplicity arises because the electron transitions involved occur without change of wavevector. For some other properties the calculation of the electronic structure is only the first step and substantial further work is needed to obtain useful results. Auger recombination is an example of that because it is necessary to consider an effective scattering of *two* carriers, involving substantial momentum transfer and the specification of *two* initial and *two* final states [6]. Impact ionization, which is the inverse process is similarly demanding to calculate [7].

The simulation of hole transport in quantum wells is another example where knowledge of the electronic structure is essential but is only one aspect of a large calculation. Intra and inter-subband scattering with substantial wavevector changes for the hole can occur as a result of a variety of phonon scattering processes. The simulation must be capable of accounting for all significant allowed processes in a complex multi-subband system and must contain an accurate description of the scattering rates for those processes. We have developed a Monte Carlo simulation in Durham

[8-9], and have used it to carry out calculations of in-plane hole transport under the action of an electric field applied to a GaAs/AlAs quantum well layer, and also to the thermalisation dynamics of excited holes in the same system. As well as being of fundamental interest, information of this kind is useful in the design of devices which require the capture and thermalisation of holes, such as the quantum well laser, and in efforts to produce fast p-channel transistors. Despite the clear usefulness of studies of hole dynamics, experimental work has been mainly directed towards electrons and there have been few realistic theoretical calculations, perhaps because of the complexity of the problem.

2. BAND STRUCTURE

The in-plane dispersion of the valence subbands of a GaAs/AlAs quantum well are markedly non-parabolic and it is important to have an accurate description of the essential features of the band structure to carry out transport simulations. We have used a complex band structure approach based on a 4-band $k.p$ scheme [5] to obtain information on the first four subbands in a 100Å wide GaAs/AlAs quantum well. Fig. 1 shows the valence band structure in the plane of the well by plotting *hole energy* against wavevector. The diagram therefore appears upside down compared to the normal representation of a valence band. Anisotropy was found to be relatively small (for example, less than 10% in band 1 in the range of the figure) and, for simplicity, the band structure was treated as isotropic in all calculations. Repulsion (anticrossing) effects between adjacent bands are clearly visible, and are accompanied by an exchange of character of the associated states. In particular, bands 2 and 4 have regions of negative effective mass near the zone centre, with energy minima at non-zero values of in-plane wavevector. The densities of states of the bands are shown in Fig. 2. Divergences are seen to occur at the energy minima, though the effect of this structure will be reduced by state broadening and band anisotropy.

Fig. 1. In-plane energy dispersion of the first four valence subbands of a 100Å GaAs/AlAs quantum well. The subbands are labelled according to the character of the zone-centre states. The energy scale is shown inverted relative to its usual form: zero energy corresponds to the base of the valence band quantum well, and energy is measured as positive in the direction of increasing subband indices.

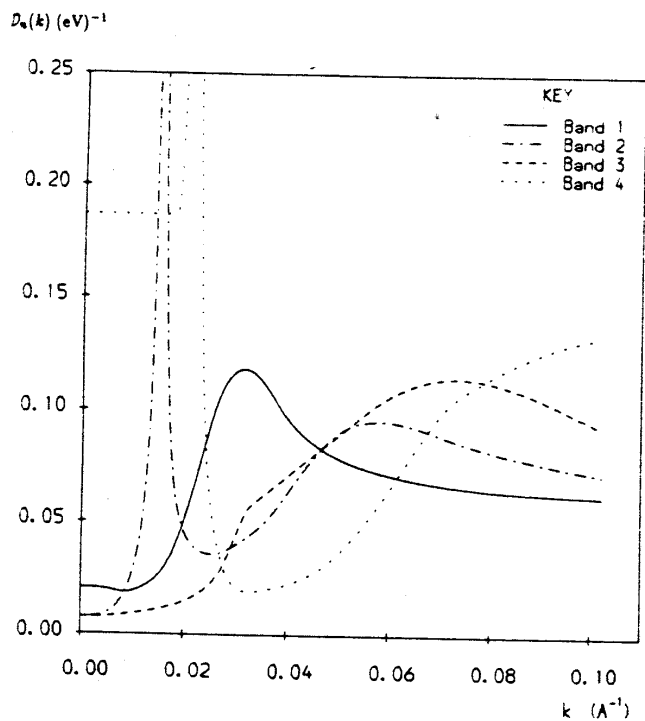
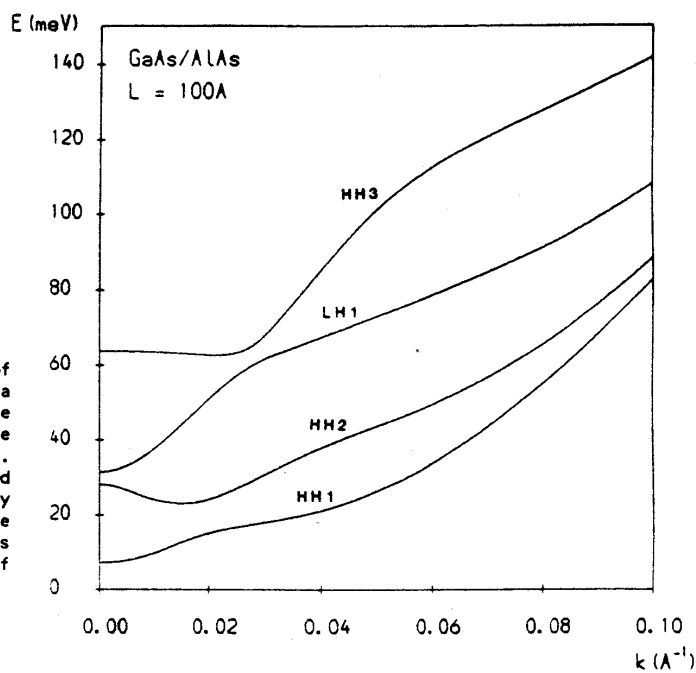


Fig. 2. Reduced density of states vs. radial wavevector in the first four valence subbands.

3. MONTE CARLO MODEL

We have developed both single particle and ensemble Monte Carlo programs [8-9] to simulate the dynamics of holes in the valence band quantum well. Using the simulations it has been possible to study the steady state transport of holes under the action of a constant, in-plane electric field; the transient behaviour of holes following the application of a field; and the relaxation of holes in the absence of field after they have been excited by some mechanism such as an optical pulse. The use of the ensemble simulation is essential for the latter two problems because of their time dependent nature.

Phonon scattering due to optical (polar and non-polar) and acoustic (deformation potential and piezoelectric) processes is included. The phonons are taken as those appropriate to bulk GaAs and phonon confinement effects resulting from the heterostructure have been ignored. Inelastic scattering for acoustic phonons is included by ascribing a fixed energy (typically 1 or 2 meV) to *all* acoustic phonons. Whilst this does not accurately reflect the acoustic phonon dispersion relation, it does provide an energy dissipation mechanism in hole relaxation simulations which would not be available if the traditional approximation of elastic scattering were employed. Ionized impurity scattering and carrier-carrier scattering have not been considered. The former could be included with little difficulty but the latter would be more problematic. The hole wavefunctions are a natural product of the band structure calculation described in Sec (2) and are used to calculate the matrix elements for hole-phonon scattering. The valence band system is modelled by the four subband dispersion curves of Fig. 1, from which group velocities and densities of states (Fig. 2) can be derived. These, and the matrix elements for the allowed scattering processes are tabulated against wavevector and are loaded into the simulation as data. The single particle Monte Carlo program typically simulates 500,000 scattering events (including self-scatterings) to determine steady state properties. The ensemble program considers some 20,000 holes in parallel, with

Fig. 3. Fractional population of holes in each of bands 1-4, as a function of in-plane electric field.

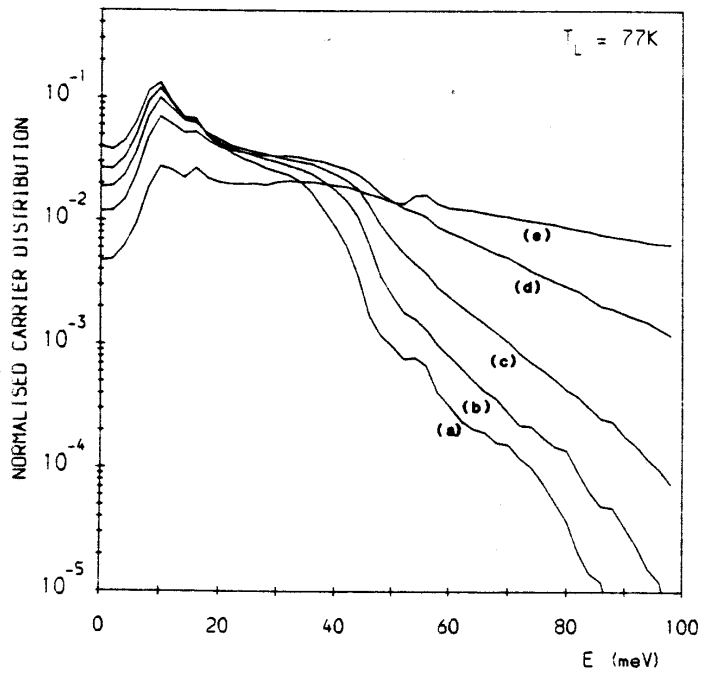
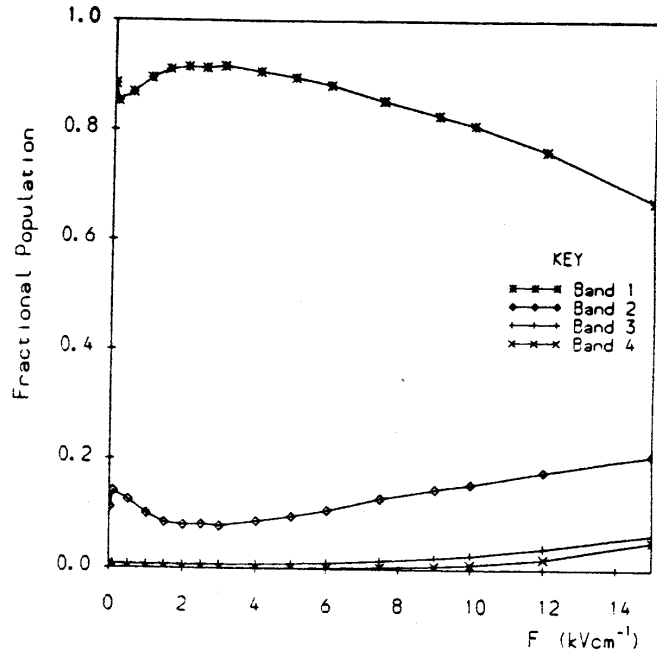


Fig. 4. Global hole energy distributions for a range of in-plane electric fields: (a) $F = 1kVcm^{-1}$, (b) $F = 2.5kVcm^{-1}$, (c) $F = 5kVcm^{-1}$, (d) $F = 10kVcm^{-1}$ and (e) $F = 20kVcm^{-1}$.

the number of scattering events determined by the duration of the time dependent process being examined.

4. RESULTS

4.1 Steady state transport in an applied field

Steady state Monte Carlo simulations of holes in a 100Å quantum well have been performed for a range of applied electric fields at a lattice temperature of 77K. Fig. 3 shows the fractional population of holes in each of bands 1-4, as a function of in-plane field. It is clear that the majority of holes reside in band 1, even at the highest field shown. Fig. 4 shows the distribution of hole energies ϵ for fields varying from 1 kVcm⁻¹ to 20 kVcm⁻¹. It is interesting to note that the maximum does not occur at $\epsilon=0$ but at $\epsilon \approx 10$ meV. This is a consequence of the form of the density of states in band 1 which is small at the band edge and has a pronounced peak at $k = 0.032\text{\AA}^{-1}$ ($\epsilon = 11.3$ meV) as can be seen in Fig. 2. The difference between the hole population at $\epsilon \approx 10$ meV and $\epsilon = 0$ increases with electric field because the heating effect of the field causes less depletion of carriers in the region of large density of states. The structure at $\epsilon \approx 16$ meV is due to the concentration of carriers in the band 2 minimum which provides a very large density of states. A similar effect is observed at $\epsilon \approx 55$ meV due to the band 4 minimum.

The drift velocities of the holes in each band as well as the overall average value are given in Fig. 5. The large values in bands 3 and 4 at intermediate fields are associated with unusually large group velocities for carriers near the energy minima, and with regions of relatively weak scattering in both bands. The negative differential mobility effects are caused by the subsequent reduction in carrier group velocities at higher energies and the eventual onset of stronger scattering in both bands. This phenomenon cannot be considered significant for device applications because the populations of bands 3 and 4 at intermediate fields are so small.

Fig. 5. Mean drift velocities for holes in bands 1-4 and the overall average hole drift velocity, as a function of in-plane electric field.

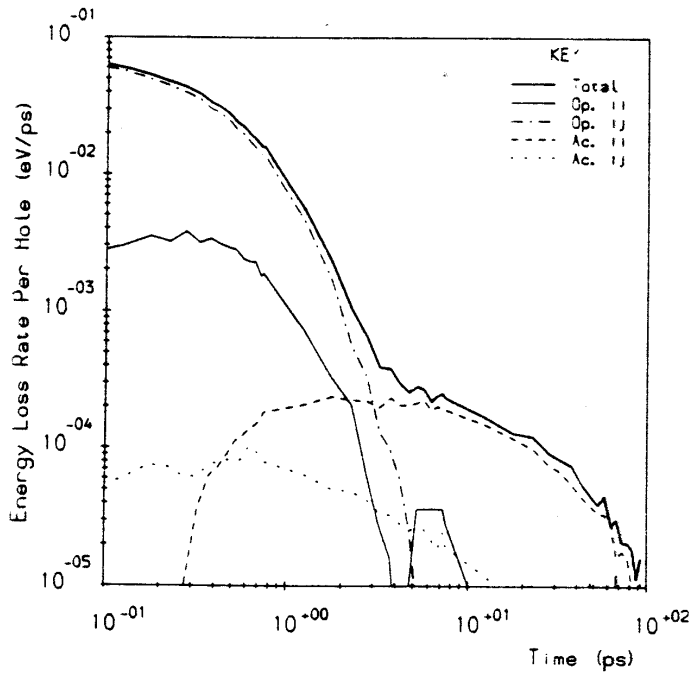
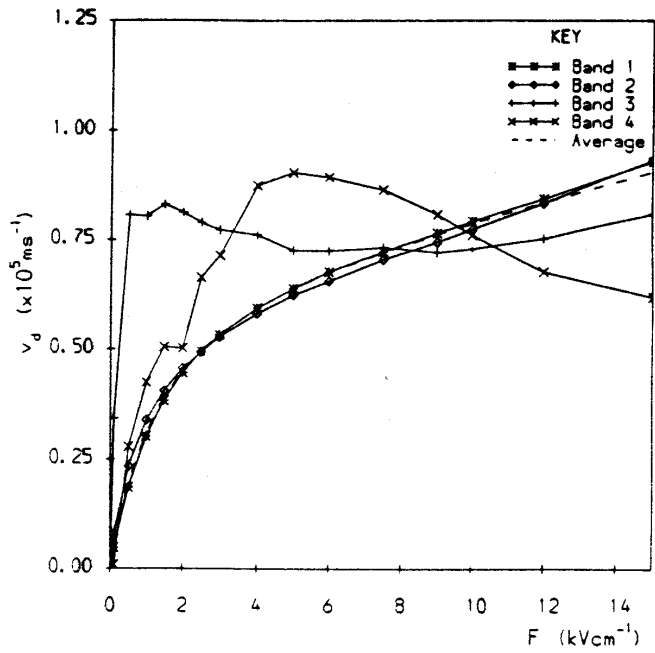


Fig. 7. Time dependence of the total hole energy loss rate and the component rates due to intraband (ii) and interband (ij) scattering via optical and acoustic modes.

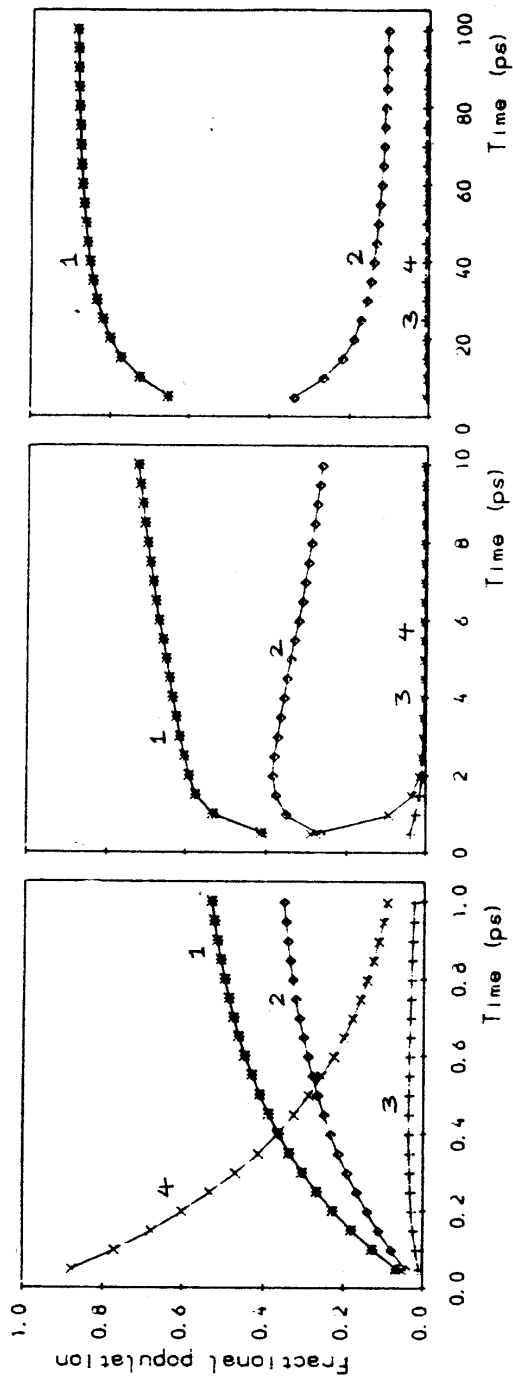


Fig. 6. Time dependence of the fractional populations in bands 1-4.

An interesting effect is seen in the response of the band 1 and 2 populations to increasing electric field. Fig. (3) shows that after an initial decrease in fractional population, band 1 experiences a repopulation so that the zero field value is exceeded throughout the low field range. One of the great advantages of the Monte Carlo simulation method is the ability to understand effects like this by examining the details of the important microscopic processes. Such an investigation shows that the reason for the repopulation effect is the difference in the rates of polar optical phonon scattering between bands 1 and 2. Scattering from band 1 to band 2 by polar optical phonon emission is suppressed because its threshold occurs at a wavevector greater than that for the equivalent intraband scattering. As a result, at the relevant applied fields, very few carriers escape intraband scattering to be transferred to band 2. Conversely, scattering from band 2 to band 1 by optical phonon emission, although relatively weak, is effective even at low fields, as soon as the carriers are accelerated up to the threshold at $k \approx 0.05\text{\AA}^{-1}$. Hence a net repopulation of band 1, relative to band 2 occurs and persists until the field is high enough to sweep band 1 carriers through the intraband scattering threshold to where interband scattering is allowed.

The simulation is capable of providing a wealth of other results on steady state phenomena, and those obtained to date are reported in detail by Kelsall [8].

4.2 Cooling of quantum confined holes

We have used the Monte Carlo simulation scheme to study the time dependent relaxation of non-equilibrium hole distributions. Again a 100Å well with a lattice temperature of 77K is considered. The nature of the initial hole distribution depends, of course, on the experiment to be modelled or the theoretical objective. Here, to illustrate the power of the technique, we describe the results for one simple situation. More details of this and other cases are described by Kelsall [8].

The initial carrier distribution is taken to be monoenergetic at the band 4 minimum. Fig. 6 shows the time dependence of the fractional populations in each band. It is seen that the majority of holes are scattered out of band 4 within the first picosecond after excitation with bands 1 and 2 showing a significant increase in population on that timescale. The dominant scattering processes during this period are polar optical phonon emissions with hole transitions from band 4 to bands 2 and 1. Band 3 is populated only very slightly since the relevant threshold for polar optical phonon emission is some 5 meV above the band 4 minimum. After $t \approx 2$ ps there is a relatively slow increase in the band 1 population, much of it at the expense of band 2. The marked change in the population transients at $t \approx 2$ ps indicates a shift from the predominance of the polar optical phonon scattering described above to acoustic phonon scattering between bands 2 and 1. In fact holes scattered into band 2 by optical phonon emission do not have sufficient energy to make a transition to band 1 by the same process, and the relatively slow acoustic phonon scattering cannot alleviate a bottleneck in carrier relaxation at the band 2 minimum.

Fig. 7 shows the average energy loss rate of the holes as a function of time, resolved into components for intra- and inter-band scattering via optical and acoustic modes. As discussed above, energy loss in the first 2-3 ps is dominated by interband optical phonon scattering. However, at $t \approx 3$ ps a crossover occurs, with energy loss dominated by intraband acoustic scattering thereafter. This acoustic scattering is largely deformation potential scattering within band 1 as the population relaxes towards the band minimum. The lack of any contribution to the energy loss rate from the intraband acoustic modes at early times ($t < 0.3$ ps) is a consequence of using an initial distribution in which all the carriers are in a band minimum. Initially, intraband acoustic scattering can only proceed via phonon absorption; hence the corresponding energy loss rate is actually negative.

5. Conclusions

We have demonstrated the use of single particle and ensemble Monte Carlo models, based on a 4-band $k.p$ band structure scheme, to simulate hole transport and relaxation in a quantum well. The complexities of the valence subband system are reflected in the hole dynamics and the hole energy distributions obtained in both steady state electric field and transient relaxation simulations. The results show the importance of using a realistic model to describe the behaviour of holes in quantum wells, and also demonstrate the potential of the model for use in the interpretation of experimental results.

Acknowledgements

R. W. Kelsall and A. C. G. Wood acknowledge tenure of SERC studentships, the latter holding a CASE studentship with Plessey Research Caswell Limited. R. I. Taylor acknowledges financial support from SERC for the period of this work.

References

1. Handbook on Semiconductors Vol 1, North Holland 1982, Editors: T. S. Moss and W. Paul.
2. Band Structure Engineering in Semiconductor Microstructures, NATO ASI Series Vol 189, Plenum, 1989. Editors: R. A. Abram and M. Jaros.
3. Y. C. Chang and J. N. Schulman 1985, Phys. Rev B31, 2069.
4. M. F. H. Schuurmans and G. W. t'Hooft 1985, Phys Rev. B31, 8041.
5. R. Eppenga, M. F. H. Schuurmans and S. Colak 1987, Phys. Rev. B36, 1554.
6. R. A. Abram, R. W. Kelsall and R. I. Taylor 1988, J. Phys Chem Solids 49, 607.
7. A. R. Beattie, 1985, J. Phys. C18, 6501.
8. R. W. Kelsall, 1989 Ph.D. Thesis, University of Durham.
9. R. W. Kelsall, R. I. Taylor, A. C. G. Wood and R. A. Abram 1989, Superlattices and Microstructures 5, 207.